Title
THEORY AND EXPERIMENTS FOR ISOTHERMAL AND NON-ISOTHERMAL SINTERING

Authors
Searcy, A.W.
Beruto, D.

Publication Date
1987-06-01

LBL-26047

Lawrence Berkeley Laboratory
UNIVERSITY OF CALIFORNIA

Materials & Chemical Sciences Division

Presented at the Conference on Science of Ceramics 14, Canterbury, England, September 7–9, 1987

Theory and Experiments for Isothermal and Non-isothermal Sintering

A.W. Searcy and D. Beruto

June 1987

Prepared for the U.S. Department of Energy under Contract Number DE-AC03-76SF00098.

DISCLAIMER

LBL-26047

THEORY AND EXPERIMENTS FOR ISOTHERMAL AND NON ISOTHERMAL SINTERING

Alan W. Searcy‡, Dario Beruto‡†

Materials and Chemical Sciences Division
Lawrence Berkeley Laboratory‡
and Department of Materials Science and Mineral Engineering
University of California
Berkeley, California 94720
Instituto di Chimica†
Universita di Genova
Genoa, Italy

ACKNOWLEDGEMENT

We thank our research collaborators R. Botter, L. Barco, P.F. Rossi, M.G. Kim, U. Dahmen and D.J. Meschi. This work was supported by the Materials Science Division, Office of Energy Research, U.S. Department of Energy.

New formulations of thermodynamics for surfaces and for non-isothermal systems are used as a basis for analyzing the kinetics of isothermal and non-isothermal sintering. The analysis suggests: 1) Rates of microstructural changes in crystalline aggregates sometimes are limited by layer growth instead of diffusion. 2) Temperature gradients can drive microstructural changes in aggregate. 3) Surface diffusion over distances much greater than particle diameters can promote densification and/or coarsening. Isothermal experiments with aggregates of very small CaO and MgO crystals suggest that coupled pore and grain growth can be a dominant process from the initiation of sintering. Densification studies with isothermal and non-isothermal aggregates confirm a significant effect of temperature gradients. Deductions from the theory and experiments are compared to observations of others.

INTRODUCTION

Essentially all theoretical models for sintering and related processes use what is for crystalline solids an approximation--that the driving force is a reduction in areas of curved surfaces of particles of isotropic surface energies. Burke,[1] Pask,[2] Johnson,[3] and no doubt others, have warned us that we should be wary of the possible consequences of this approximation. Crystalline particles often have anisotropic surface energies and

may develop facets during sintering at the cost of an increase in surface area[4] Fig. (1).[5] How our neglect of such facts may influence deductions from theory has not been known.

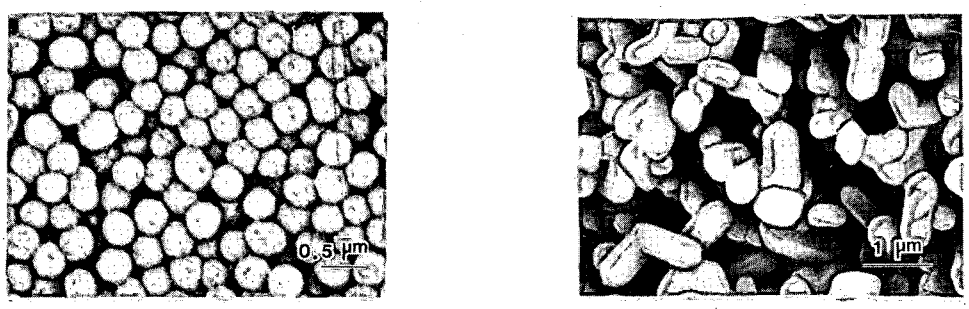

Fig. 1 Rutile particles before (left) and after(right) sintering in HCl at 1000°C.[5]

Sintering theories also include the implicit assumption that temperature gradients provide no significant driving force. But there is clear evidence that temperature gradients drive segregation in solids[6-7] and that temperature gradients cause pores to migrate.[7,8] Figure (2) shows dramatic changes that were produced in a bar of Ba-Cu-Y-O superconductor of initial 50% porosity when held for 16 hours in a gradient between 950°C and 500°C.[9] In light of such evidence that temperature gradients cause mass transport in solid phases, we should expect that temperature gradients will sometimes provide an important driving force for sintering.

New evaluations of the conditions for maximum stability for crystalline particles[10,11] and for solids in temperature gradients[12] now make it possible to predict the influence of anisotropic surface energies and of temperature gradients in

(Y,Ba,Cu)Oxide (123) powder compact held in air for 16 hrs in temperature gradient

930 C 830 730 560

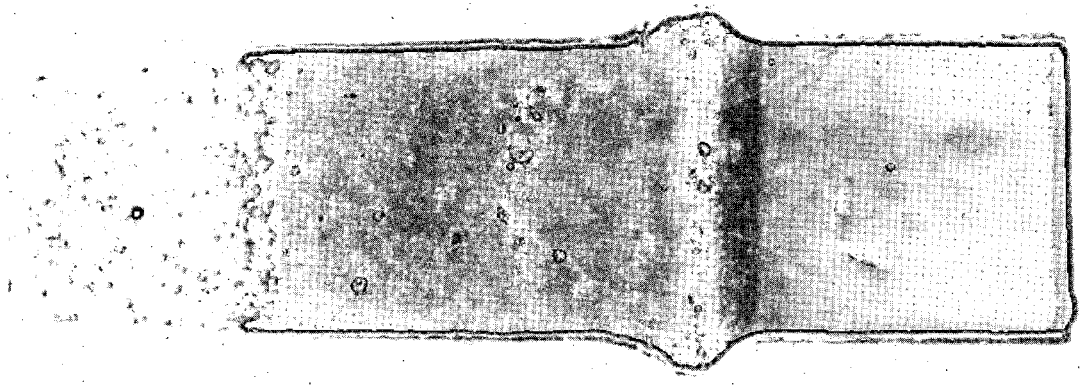

I I I I

(x,y,z) (1,1,1) (1,2,3) (1,2,4) (1,2,3) Y_x Ba_y Cu_z

3 mm

Fig. 2. Partitioning of $y_1Ba_2Cu_2O_n$ superconductor in a temperature gradient.[9]

driving surface area changes, pore elimination, and grain growth.[13-15] A section on theory outlines the analysis and its conclusions. Studies in our Laboratories which were designed to test sintering theories with exceptionally well characterized crystalline oxide powders under isothermal and non-isothermal conditions are described in an experimental section. In a discussion section it is argued that the data obtained in those studies, experimental data of others, and the new theoretical models suggest that some ideas about sintering should be re-evaluated.

THEORY

Thermodynamics of Isothermal Particles

Most ceramics contain two or more chemical components. But for simplicity, kinetic and thermodynamic expressions will be developed only for phases that contain a single atomic species and vacancies. The major kinetic and thermodynamic deductions reached below would be unchanged for a multicomponent solid in which sintering occurs at constant composition.

We first seek an expression for the flux of atoms which move from n_i sites at a particular temperature and with a particular bonding environment to n_j adjacent sites where the bonding environment is different.[10] The probability that any particular atom on an n_i site will be adjacent to a vacant j site is the product of the mole fraction of i sites that are occupied, X_i, and of j sites that are vacant, X_{vj}. To be converted to a j atom and i vacancy pair, the initial molecule-vacancy pair must

acquire a thermal free energy $G_i^* - G_i^t - G_{vj}^t$, where G_i^t is the thermal free energy of the i atom, and G_{vj}^t is that of the j vacancy. Then the total flux from n_i to the j collection is

$$J_{ij} = n_i \nu_{ij} g_{ij} X_i X_{vj} \exp\left(- \frac{G_i^* - G_i^t - G_{vj}^t}{kT} \right) \qquad (1)$$

where ν_{ij} is the frequency with which an atom-vacancy pair is excited to the free energy G_i^*, and g_{ij} is the probability that the excited i atom and j vacancy pair will move in the direction in physical space that transfers the molecule and vacancy across the free energy barrier G_i^*. The flux from n_j to n_i is given by a similar expression with the subscripts reversed. Eq. (1) should be valid for any adjacent rows or layers of a crystalline particle.

At equilibrium, $J_{ij} = J_{ji}$, terms in $n\nu g$ cancel, and by microscopic reversibility $G_i^* = G_j^*$. Therefore,

$$\frac{X_i}{X_{vi}} \exp\left(\frac{G_i^t - G_{vi}^t}{kT} \right) = \frac{X_j}{X_{vj}} \exp\left(\frac{G_j^t - G_{vj}^t}{kT} \right) \qquad (2)$$

Eq. (2) can be put in the equivalent form

$$\frac{n_i}{n_{vi}} \exp\left(\frac{G_i^t - G_{vi}^t}{kT} \right) = \frac{n_j}{n_{vj}} \exp\left(\frac{G_j^t - G_{vj}^t}{kT} \right) \qquad (2')$$

In a particle with more than two different bonding environments, dynamic equilibrium requires that an equation like Eq.(2) characterize the vacancy distribution between each separate pair of environments. This generalized form of Eq.(2) can also be derived[11] from the requirement

$$\delta G = \delta \sum (G_i n_i + G_{vi} n_{vi}) \geq 0, \qquad (3)$$

where the minimum is taken with respect to changes in shape and with respect to the exchange of atoms and vacancies between sites of different bonding environments.

Classical surface thermodynamic theory accounts for the increased chemical activities of small particles by introducing the assumption that surfaces are under tension (for liquids) or stress (for solids).[16] That assumption of classical theory is not needed to account for the influence of surfaces on the stabilities and related properties of particles when it is recognized that minimization of particle free energy demands that vacancies be redistributed.[11] The vacancy concentrations in each sub-part of a crystal which makes the free energy a minimum depends through Eq.(3), not only on the local bonding environment, but on the relative numbers and bonding environments of all sites of the crystalline particle. The smaller the crystal of a given composition, the smaller becomes X_{vb}, the vacancy concentration on bulk lattice sites. But always,

$$\frac{X_b}{X_{vb}} \exp\left(\frac{G_b^t - G_{vb}^t}{kT}\right) = \frac{P}{PX^o} \exp\left(\frac{G_g}{kT}\right) \qquad (4)$$

where P is the vapor pressure in equilibrium with the particle, PX^{o} is the standard pressure, and G_g is the standard free energy of the vapor. Because X_{vb} decreases as the particle size decreases, the vapor pressures of small crystals are increased. For liquids, partitioning of molecules and free volume between bulk and surface regions of drops can cause a similar size effect on properties.[11]

Eq. (3) is in principle exact (though the values of some of the terms in the summation may be unavailable). If only nearest neighbor bonds are significant, so that surface free energies are associated with monolayers, and if the small reduction in free energy that results from vacancy partitioning is neglected Eq. (3) becomes in terms of macroscopic variable

$$\delta\sum(\sigma_i A_i + \gamma_i h_i) \geq 0 \qquad (5)$$

for any changes in shape or vacancy distribution, where σ_i is the unit free energy of a surface of area A_i, γ_i is the unit free energy of an edge or a ledge, and h_i is its length. Ledges, and kinked ledges, may be present in a particle of minimum free energy content because a crystal of arbitrary number of atoms with the optimum number of vacancies will usually not have the exact number of sites required for a perfect crystal shape.

When edge effects are neglected, Eq. (5) reduces to

$$\delta\sum\sigma_i A_i \geq 0 \qquad (6)$$

which is the condition deduced by Gibbs[16] and Curie[17] to describe equilibrium shapes of faceted crystalline particles. Herring[18] showed that Eq. (6) can be generalized to describe equilibrium

crystals which are bounded by a combination of planar and rounded surfaces. But its neglect of edge effects makes Eq. (6) inadequate for analysis of the kinetics of particle shape changes. Kinetic analysis requires the use of Eq. (3) or (5).

Isothermal Kinetics

Many years ago Herring[19] pointed out that the sintering of crystalline solids might sometimes be limited not by diffusion, but by the rate at which new crystal layers are nucleated or grow. Coble and Cannon[20] and Johnson[3] analyzed the influence of a slow step of vacancy formation or annihilation at a surface or interface. Here, the kinetics of ledge growth is examined for three simple cases in terms of Eq. (3) or (5).

Suppose, for example, that a closed pore can decrease in volume because of diffusion to it of atoms from a surface layer. The driving force for transfer of atoms from the outer surface to the surface of a pore is the free energy decrease that results because atoms of a pore surface--on average--form more bonds than do atoms of an outer surface. To illustrate this point, suppose both the outer surface layer and the surface layer of the pore are close packed and that only nearest neighbor bonding is important, assume additivity of nearest neighbor bonds, and neglect entropies.

There is no barrier to nucleation of a new row of atoms on a perfect low index surface of a pore because an atom placed in one of the corners on that surface has as many neighbors, 6, as an

atom at a corner or kink site of an outer surface layer. The free energy of the bonds formed by an incomplete edge row of n_i atoms on a pore surface is $H_b[7(n_i-1)+6]$, where H_b is the enthalpy of a nearest neighbor bond. The free energy of bonds of the n_o atoms in an outer surface edge row is $H_b[7(n_o-2) + 2\times6]$. The <u>average</u> free energy change <u>per atom</u> when n_i atoms are transferred from an outer surface edge row for which $n_o >> n_i$ to form a new edge row of a pore is $\delta G = - H_b/n_i$.

Classical sintering theories treat this free energy of transfer as a continuum, which implies that $\delta G/\delta n$ has the same value for every atom transferred. But for crystalline solids, most transfers between outer surface corner or kink sites to kink sites of pores are thermodynamically neutral in the sense that the average number of bonds per atom is unchanged. Only transfers that remove the last atom of an outer surface row or introduce the last atom of an inner surface row are thermodynamically favorable to pore closure. Fig. (3) illustrates the problem in a 2-dimensional model.

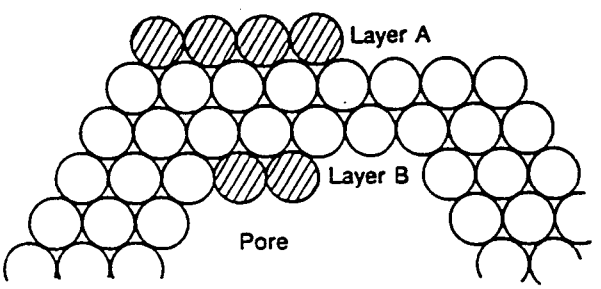

For transfer of one or two atoms from B to A, $\delta G \cong 0$
For transfer of one atom from A to B, $\delta G \cong 0$
But for transfer of two atoms from A to B, $\delta G < 0$

Fig. 3 Illustration of zero and negative free energy changes in crystals.[13]

In three dimensions the problem is to calculate the rate at which a new row of n_i atoms can be added to an inner surface by random additions--or losses--of atoms from kink sites. In a model calculation[21] loss of atoms from a completed row of a pore is assumed to be negligible, but transfer of the n_i atoms to form a row must occur despite the fact that atoms or vacancies of the source have the same activities as atoms or vacancies at the sink. The expression for the steady-state atomic diffusion flux J in a two step irreversible process when the activity is defined as unity is

$$J = \frac{k_1 k_3}{k_2 + k_3} \tag{7}$$

where $k_1 = k_2 = A_e D/q$, the effective area A_e for diffusion times the diffusion coefficient D divided by the distance q to the pore, and k_3 is the rate of the growth step. Here k_3 is not a usual rate constant, but the probability that random movements of atoms in the self adsorption layer of the pore will form a new row of n_i atoms. This probability is estimated to be

$$n_i \nu X_a (1/n_i)^2 \exp(- G_m^*/kT) \tag{8}$$

where ν is an attempt frequency X_a is the fraction of occupied sites, $(1/n_i)^2$ describes the statistical fluctuation required to fill a row, and G_m^* is an activation energy for movement. Using the nearest neighbor approximation to estimate terms in Eq. (8) with a reduced bond energy of $H_b/kT = 3.3$ at 1000 K yields $k_3 = 0.03/n_i$. So, if the cross sectional area for diffusion is

assumed to be n_i^2 and if D = 10^{-8} cm/sec and q = 10^{-4}, ledge growth would be slower than diffusion for pores with cross sections greater than about 7 atoms, or 20 nm. This estimate must be recognized as uncertain by orders of magnitude. But the calculation shows that the smaller the pore, the shorter the time until a statistical fluctuation from equally probable energy states completes a row. The rate of the pore closure should increase, therefore, with decreasing pore cross section.

In the neck region between crystalline particles the boundary along which the two particle surfaces intercept provides a line at which formation of a new surface layer of each grain is favored by bonding across the interface with atoms of the other grain. Consequently, surface layers that terminate at necks can grow by transfer of atoms from edge rows of outer surfaces, which have, on average, fewer bonds. Because each successive new layer of atoms added to a crystal surface near a neck is nucleated at a successively later time, the later layers extend shorter distances from the grain boundary,and the necks may appear rounded at low magnifications despite the fact that they are formed from stepped low index layers.

If, as usually assumed, exaggerated grain growth is driven by surface curvature, the direction of boundary movement should always be towards the center of curvature of the grain boundary along which growth occurs.[1] But De Jonghe[22] has shown by high resolution TEM that Na β''-alumina grows by the addition of planar ledges of 1.13 nm in height, with no liquid phase present; The

ends of these tabular grains sometimes are curved in a direction opposite to that expected from the theory. Such observations are easily explained if we assume that exaggerated grain growth is not driven by curvature, but by changes in interfacial energies.

Exaggerated grain growth is usually favored by a reduction in the concentration of line defects which accompanies the process, but this effect can be neglected here. The free energy content for the collection of small grains is $G_V = \sigma_S A_{VS}$ where σ_S is their average grain-boundary free energy per unit area, and A_{VS} is their grain-boundary area per unit volume (with that volume large enough to contain many small grains). For advance of a unit area of the large grain boundary upward by a distance δq

$$\delta G_V = - (\sigma_S A_{VS}) \delta q \qquad (9)$$

Eq. (9) predicts that exaggerated grain growth is driven principally by reduction in area of small grain boundaries when a differential volume element is swept out by the growing grain.

The model explains convex, concave and planar boundaries during exaggerated grain growth as consequences of relative rates of nucleation and growth of new crystal layers.[14]

The Kinetics of Non-isothermal Sintering

An equation for the flux of atoms from sites at a temperature T_i to sites at a different temperature T_j can be obtained by modifying Eq. (1), to introduce local site temperatures and the temperature T* of the transition state.[12,15] When the flux J_{ij} is set equal to J_{ji} the non-thermodynamic terms cancel as before.

A single phase solid in a temperature gradient, therefore, would be in a state of maximum stability when the relationship between its sub-parts is

$$\frac{X_i}{X_{vi}} \exp\left(\frac{G_i^t - G_{vi}^t}{kT_i}\right) = \frac{X_j}{X_{vj}} \exp\left(\frac{G_j^t - G_{vj}^t}{kT_j}\right) \qquad (10)$$

Eq. (10) can also be derived by assuming that the condition for maximum stability of a solid in a temperature gradient is that the ratio of its Gibbs free energy in each volume element to the local temperature of that volume element is a minimum, that is

$$\sum \frac{(n_i G_i + n_{vi} G_{vi})}{kT_i} \text{ is a minimum} \qquad (11)$$

For an initially one-component or pseudo-one-component solid the minimum value of Eq.(11) is obtained when the solid has moved to form a pore-free mass in the subvolume of lowest temperatures. If the temperature gradient does not change the vacancy concentrations from the values characteristic of equilibrium at the local temperatures, the driving force for transport from a higher temperature T_i to a lower temperature T_j can be written as

$$\frac{P_i - P_j}{PX^o} = \exp\left(-\frac{\Delta G_i}{kT_i}\right) - \exp\left(-\frac{\Delta G_j}{kT_j}\right) \qquad (12)$$

where P_i and P_j are vapor pressures, PX^o is the standard pressure and ΔG_i and ΔG_j are free energies of vaporization.

Because the stability of the condensed phase can be increased by a shift of vacancies from the higher temperatures towards the lower, the driving force in a temperature gradient may be increased over the value predicted by Eq. (12).[12] This shift in vacancies would increase the driving force by increasing P_i and would increase the probability of atom-vacancy exchanges in the lower temperature range.

For silver or MgO, a 1°C/mm temperature gradient is calculated to influence local pressure differences more than do surface energy gradients for particles of radii >30 μm.[15] The driving forces provided by temperature gradients and by surface energy changes are additive. Therefore, as long as open channels are present, vapor phase or surface diffusion can cause densification in temperature gradients by transporting matter from hotter parts of a porous aggregate to cooler parts. There, because of the influence of surface geometry, growth in neck regions would occur preferentially.

But unless the minimum temperature in the gradient is maintained high enough to transport matter to the coldest parts in the time provided, the temperature gradient will cause differential densification or coarsening.

EXPERIMENTAL

Isothermal Studies

CaO, obtained from decomposition of $CaCO_3$, and MgO, obtained by decomposition of $MgCO_3$ or $Mg(OH)_2$, are exceptionally valuable materials for use in testing theories about early stages of sintering.

The CaO produced by vacuum decomposition of $CaCO_3$ is formed as aligned rod-shape particles of normal, NaCl-type CaO which are approximately 10 nm (100 Å) in diameter.[23] The combined use of condensation of liquid N_2 in pores, H_g porosimetry, and micrometer measurements of dimensions of mm size particles provides a complete accounting of the pore size distribution in the CaO aggregates.[24] Surface areas are available from BET measurements. The CO_2-catalyzed sintering of this CaO has been studied in an apparatus in which the weight changes produced by CO_2 sorption at high temperatures and by N_2 adsorption at 73 K both can be measured without exposure of the CaO to the atmosphere.[25]

MgO from $Mg(OH)_2$ decomposition is formed as orthorhombic boxes in aggregates of about 54% porosity. The aggregates are essentially perfectly aligned, so that an electron micrograph pattern is like that of a single crystal.[26] Calorimetric measurements show the total surface area of these aggregates to be 950 ±100 m^2/g.[27] BET measurements show only 100 to 300 m^2 surface per gram to be accessible to N_2; the accessible surface decreases with particle size of the source $Mg(OH)_2$.[28] The calorimetric estimate is confirmed by direct TEM observations of total area which show particles of nearly square cross sections and 1 nm to 2 nm edge lengths.[26,29] From these cross sections the surface area is calculated to be > 800 m^2/g.

Changes in surface areas and pore volumes which resulted from sintering the CaO were studied first.[25] Average pore cross sections Fig. (4) were calculated from the data on the assumption

that the pores retain a tubular geometry during sintering. This basic geometry was confirmed by SEM observation. The data show that pore and particle growth begin as soon as bulk or grain boundary diffusion begins.

Grain growth is known to occur during initial and intermediate stages of sintering,[30-32] but Exner and Petzow[33] apparently expect negligible grain growth in a regular array of equally spaced particles, and Lange[34] suggests growth is important only in volume elements where the local density is nearly 100%. The data for CaO suggest that pore and grain growth can occur in aggregates of uniform packing of similar particles. The N_2 measurements are sensitive only to areas and volumes of the particles and pores of < 100 nm cross section, and these were uniform in size and spacing.

When aggregates of the aligned particles of MgO were sintered in water vapor at 823 K, stronger evidence was obtained that coupled pore and grain growth is a dominant process from the initiation of sintering in aggregates of uniform particle and pore dimensions. Figure (5) shows on the left hand scale the decreases in pore volume and area that began when water vapor was introduced. The right hand scale shows the changes in the cross section of pores which were on the assumption that the pores were tubes of square cross sections. The basic conclusion from the figure, that the average cross section of pores began to increase as soon as sintering was initiated, depends only on the section of pores which were on the assumption that the pores were tubes of square cross sections. The basic conclusion from the

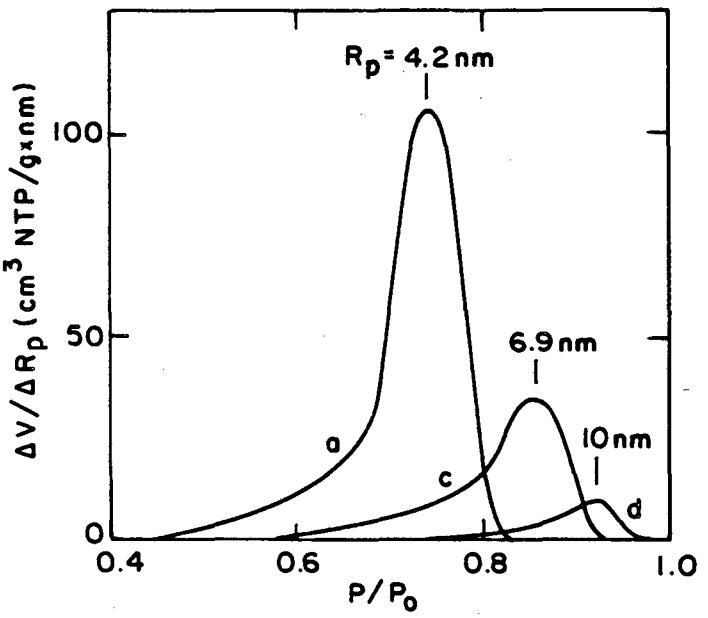

Fig. 4 Pore cross sections in CaO.[25]

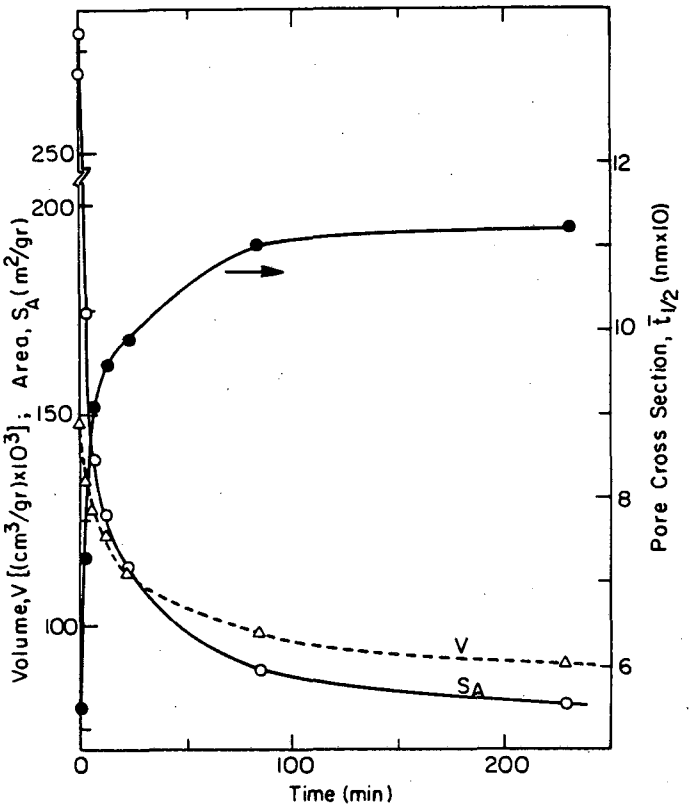

Fig. 5 Pore cross sections in MgO.[27]

section of pores which were on the assumption that the pores were tubes of square cross sections. The basic conclusion from the figure, that the average cross section of pores began to increase as soon as sintering was initiated, depends only on the assumption that the average cross section changes in a regular manner with sintering. TEM pictures of the sintered MgO look like higher magnifications of the original particles and pores.

A plot of the excess energy measured calorimetrically for MgO against surface areas accessible to N_2[27] provides another interesting finding. If diffusion were rate limiting, the H_2O-catalyzed surface diffusion of MgO would be expected to cause the surface areas accessible to H_2O gas to decrease more rapidly than the areas of closed pores. If so, after N_2-accessible surface

areas were reduced by sintering, the heats of solution would still remain high because those heats measure the energies of closed pores as well as open pores. But small initial reductions in N_2-accessible area produced large reductions in measured heats. Closed pores must have been eliminated at a faster rate than open pores, despite the fact that bulk diffusion is required for closed pore elimination. This observation can be understood in terms of the theory outlined in the section on isothermal sintering. If layer growth steps are rate limiting, closed pore elimination would be favored over elimination of open pores because bonding interactions along all edges of a new layer of a closed pore are favorable and because the closed pores in the MgO studies were smaller than the open pores.

Non-Isothermal Experiments

For non-isothermal studies,[35] aggregates of aligned MgO particles were sintered in water vapor until the surface area was reduced to 8 m^2/g. Particle cross sections were estimated from SEM photographs to be 100 to 200 nm. The material had an apparent density of about 3.5 g/cm^3, close to the theoretical density, which implies that closed pores are absent. The MgO was formed into compacts with green densities of 0.7 to 0.9 g/cm^3.

For reference, some runs were made in a part of the furnace where the temperature was isothermal to ± 2°. Non-isothermal runs were made in a part of the furnace where the temperature varied almost linearly. Data for the non-isothermal samples were corrected for linear shrinkage by assuming that all the shrinkage

was toward the hot end. This method of analysis underestimates the influence of a temperature gradient; transport should be toward the colder end of the gradient so that the maximum temperature of the gradient decreased as a sample shrank. Two sets of experiments will be cited.

Three samples with similar green densities were compared after sintering for about 110 min. Sample a was held at 1300 ±2 K , sample b in a gradient from 1299 ±2 K to 1213 ±2 K and sample c was held at 1213 ±2 K. Plots of fired densities vs green densities were used to correct samples to equivalent initial densities. Corrected densities for samples a, b, and c were then .93, .90 and .77. The density predicted for the sample in the temperature gradient on the assumption that the density would be an exponentially weighted average of those measured in the isothermal runs[36] is 0.81. A striking observation was that the radial shrinkage of sample b is 9.7% at its hot end compared to 6.2% for the hotter isothermal sample and is 3.4% at its colder end, compared to 0.7% for the colder isothermal sample.

Figure (6) shows the effects on density of 150 min heat treatments at 1303 K and in a gradient between 1303 K and 1233 K. Densities were measured for 1 mm sections in the first 6 mm of a sample and for the final 4 mm section. For 2 specimens held in the temperature gradient, densities averaged higher for the hottest third of the samples than for the isothermal 1303 K sample and averaged lower than it in the coldest third. The exponentially weighted average density calculated for the non-

isothermal specimens on the assumption that isothermal kinetics applies is 0.93 g/cm^3, significantly lower than measured densities even in the coldest third of the samples.

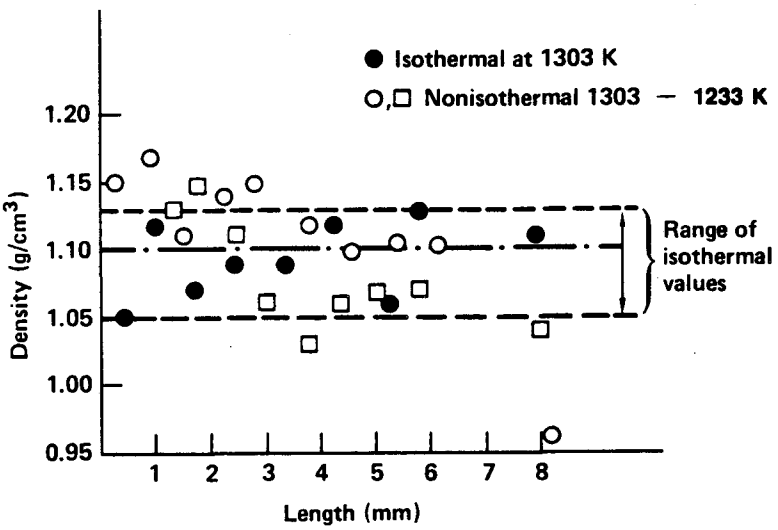

Fig. 6 Density variations in 10mm bar. Expected average density if isothermal kinetics applied in the gradient is 0.93 g/cm^3.[35]

DISCUSSION

Kinetics of Isothermal Sintering

Model experiments with relatively large metal spheres or metal wires give direct experimental support to the view that models for densification can neglect grain growth as long as channels remain open in an aggregate.[37,38] But our isothermal experiments suggest that in uniform aggregates of exceptionally small particles grain growth occurs from the initiation of sintering. What then is the probable role of grain growth when particles are in the range of usual ceramic interest?

Whittemore and Sipe[31] used Hg porosimetry to measure changes in pore size distributions from the initiation of sintering for a number of oxides. One was MgO in which the initial pores grew by

a factor of 5 to about 400 nm cross section as the cumulative pore volume decreased by about a factor of three.

Barringer et al[39] evaluated grain growth during densification of monodispersed rutile crystals of 300 nm initial cross sections, uniformly packed, with relative green densities of 55%. By the time that the relative density reached 93%, the number of particles was reduced to one-eighth the original number. The number of pores must also have decreased.

Kolar et al[40] have provided strong evidence that pore growth occurs by Ostwald ripening in later stages of sintering. Models should be explored which assume pore and grain growth by a near-equilibrium Ostwald ripening to be the dominant process from the initiation of sintering, with shape changes, coarsening, and densification competing processes superimposed on the growth. The possibilities that ledge nucleation or ledge growth may limit the rates and that densification and/or coarsening are produced by transport over distances of many particle diameters should be evaluated.

Non-Isothermal Sintering

The beneficial effects of fast firing reported by Vergnon, et al[41] and others[42-45] and of rate controlled sintering[46] in increasing densification rates and reducing grain growth may be primarily consequences, not of heating rates per se, but of temperature gradients. We can hope that, in a suitably chosen gradient, matter will diffuse by vapor transport and by surface diffusion from the hottest part of the specimen to the coldest

part to fill in pores with little grain growth. Gradients may also cause beneficial particle rearrangements as suggested by Lis, et al.[45] But when the coldest part of a specimen is too cold, differential densification of the kind illustrated by Figure (6) will result, because diffusion rates limit mass transport to the coldest part.

For good or evil, temperature gradients must significantly influence the microstructural changes that occur during the firing of commercial ceramic objects. In commercial operations[47] heating rates are fast, and specimens are usually much larger than laboratory specimens. Large temperature gradients can be expected during much of the firing cycle. If ceramic science is to provide better guidance to engineering practice, we must clarify the influence of these gradients.

REFERENCES

1. BURKE, J.E., in: Chemical and mechanical behavior of inorganic materials (Eds.: A.W. Searcy, D.V. Ragone & U. Colombo). New York: Wiley-Interscience (1970).

2. PASK, J.A., Proc. int. symp. on factors in densification and sintering of oxide and non-Oxide ceramics, Japan, 580 (1978).

3. JOHNSON, D.L., Mater. Sci. Res., 13, 97, 1980.

4. KUMAR, P. & JOHNSON, D.L., J. Am. Ceram. Soc., 57, 62, 1974.

5. EDELSON, L.H. & GLAESER, A.M., J. Am. Ceram. Soc., submitted.

6. SCHMALZRIED, H., LAQUA, W. & LIN, P.L., Z. Naturfosch., 34a, 192, 1979.

7. OLANDER, D.R., Fundamental aspects of nuclear reactor fuel elements, Oak Ridge, TN: Energy Research and Development Agency (1976)

8. LEMAIRE, P.J. & BOWEN, H.K., J. Am. Ceram. Soc., 65, 49, 1982.

9. RAHAMAN, M.N. & DE JONGHE, L.C., unpublished work.

10. SEARCY, A.W., J. Chem. Phys., 81, 2489, 1984.

11. SEARCY, A.W., J. Chem. Phys., 83. 3095, 1985.

12. SEARCY, A.W., Lawrence Berkeley Lab.-23229 (1987).

13. SEARCY, A.W., J. Am. Ceram. Soc., 68, C-267, 1985.

14. SEARCY, A.W., J. Am. Ceram. Soc., 69, C-91, 1986.

15. SEARCY, A.W., J. Am. Ceram. Soc., 70, C-61, 1987.

16. GIBBS,J.W.,The scientific papers. Vol. 1, thermodynamics, New York: Dover (1961).

17. CURIE, P., Bull. Soc. Min. France, 81, 145, 1885.

18. HERRING, C., Phys. Rev. 82, 87, 1951. 19. HERRING, C., in: Structure and properties of solid surfaces (Eds.: R. Gomer, C.S. Smith) Chicago: University of Chicago Press (1953).

20. COBLE, R.L. & CANNON, R.M., Mater. Sci. Res., 11, 151, 1978.

21. SEARCY, A.W., MESCHI, D.J. & BERUTO, D., Lawrence Berkeley Lab.-23919 (1987).

22. DE JONGHE, L.C., unpublished microstructures associated with J. Am. Ceram. Soc., 62, 289, 1985.

23. TOWE, K.M., Nature, 274, 239, 1978.

24. BERUTO, D., BARCO, L. & SEARCY, A.W., J. Am. Ceram. Soc., 66, 893, 1983.

25. BERUTO, D., BARCO, L. & SEARCY, A.W., J. Am. Ceram. Soc., 67, 512, 1984.

26. KIM, M.G., DAHMEN, U. & SEARCY, A.W., J. Am. Ceram. Soc., 70, 146, 1987.

27. BERUTO, D., ROSSI, P.F. & SEARCY, A.W., J. Phys. Chem. 89, 1695, 1985.

28. BERUTO, D., BOTTER, R. & SEARCY, A.W., J. Am. Ceram. Soc. 70, 155 1987.

29. MOODIE, A.F. & WARBLE, C.E., J. Cryst. Growth 74, 89, 1986.

30. MORIYOSHI, Y. & KOMATZU, W., J. Am. Ceram. Soc., 53, 671, 1970.

31. WHITTEMORE, O.J., JR & SIPE, J.J., Powder Tech., 9, 159, 1974.

32. WHITTEMORE, O.J. & VARELA, J.A., Mater. Sci. Res., 13, 51, 1980.

33. EXNER, H.E. & PETZOW, G., Mater. Sci. Res., 13, 107, 1980.

34. LANGE, F.F., J. Am. Ceram. Soc., 67, 83, 1984.

35. BERUTO, D., BOTTER, R. & SEARCY, A.W., unpublished work.

36. VENKATU, D.A. & JOHNSON, D.L., J. Am. Ceram. Soc., 54, 641, 1971.

37. KUCZYNSKI, G.C., J. Appl. Phys., 21, 632, 1950.

38. GERMAN, R.M. & MUNIR, Z.A., J. Mater. Sci., 10, 1719, 1975.

39. BARRINGER, E.A., BROOK, R. & BOWEN, H.K., Mater. Sci. Res., 16, 1, 1984.

40. KOLAR, D, KUCZYNSKI, G.C. & CHIANG, S.K., Mater. Sci. Res., 16, 81, 1984.

41. VERGNON, P., JUILLET, F., ELSTON, J. & TEICHNER, J.J., Rev. Hautes Temper. et Refract., 1, 27, 1964.

42. IVENSEN, V.A., Sci. of Sintering, 10, 175, 1978.

43. MORELL, A. & HORMOSIN, A., Am. Ceram. Soc. Bull., 59, 626, 1980.

44. HARMER, M.P. & BROOK, R.J., J. Br. Ceram. Soc., 80, 148, 1981.

45. LIS, J., PAMPUCH, R. & GASIOREK, W., Sci. of Ceramics 12, 327, 1984.

46. HUCKABEE, M.L., HARE, T.M., PALMOUR, H. III, Mater. Sci. Res., 11, 205, 1978.

47. KOLAR, D., Mater. Sci. Res., 13, 335, 1980.

LAWRENCE BERKELEY LABORATORY
TECHNICAL INFORMATION DEPARTMENT
UNIVERSITY OF CALIFORNIA
BERKELEY, CALIFORNIA 94720